Optics & Laser Technology 197 (2026) 114767

Contents lists available at ScienceDirect

Optics and Laser Technology

journal homepage: www.elsevier.com/locate/optlastec

Full length article

Sensing changes in triglyceride concentration in blood solution using diffuse optical spectroscopy

Siqi Liang [a,b,1], Nan Wan [b,1], Guo Chen [b,1], Sung-Liang Chen [b,c,d,*], Myeongsu Seong [e,**]

[a] School of Information and Electrical Engineering, Hunan University of Science and Technology, Xiangtan 411201, China
[b] Global College, Shanghai Jiao Tong University, Shanghai 200240, China
[c] Institute of Medical Robotics, Shanghai Jiao Tong University, Shanghai 200240, China
[d] Engineering Research Center of Digital Medicine and Clinical Translation, Ministry of Education, Shanghai 200300, China
[e] Department of Mechatronics and Robotics, School of Advanced Technology, Xi'an Jiaotong–Liverpool University, Suzhou 215123, China

ARTICLE INFO

Keywords:
Triglyceride
Cardiovascular disease
Hypertriglyceridemia
Diffuse optical spectroscopy
Noninvasiveness

ABSTRACT

Triglyceride (TG) is a fundamental lipid component in the bloodstream. While TG is fundamental in the body, elevated TG levels, exceeding 150 mg/dL, pose a heightened risk for multiple diseases, notably cardiovascular disease. Monitoring TG concentration is imperative to assess the efficacy of interventions aimed at lowering the TG concentration and diagnosing hypertriglyceridemia (HTG, TG concentration $\geq$ 200 mg/dL). Although various techniques exist for TG concentration monitoring, conventional techniques often require sample collection and/or sample preprocessing or lack portability. Recognizing the importance of TG concentration monitoring, this work endeavors to explore the viability of diffuse optical monitoring of TG concentration variations in blood. To validate the feasibility, a series of Monte Carlo simulations was performed. Then, samples containing flowing mixtures of varying TG concentrations and hemoglobin solution (for phantom experiments) or sheep blood (for *ex vivo* experiments) were measured using continuous-wave diffuse optical spectroscopy (CW-DOS) to experimentally demonstrate the capability of diffuse optical monitoring of TG concentration variations. Our results showed a linear decrease in CW-DOS amplitude at 885 nm with increasing TG concentration up to 800 mg/dL. In addition, *in vivo* mouse studies were conducted, including a control group receiving saline (n = 5) and a test group administered triton WR-1339 (n = 5), to further demonstrate the applicability of the technique. Our results suggest that CW-DOS holds promise as a noninvasive and longitudinal tool for monitoring TG concentration, facilitating the diagnosis of HTG and the assessment of the efficacy of interventions aimed at reducing TG levels in individuals.

1. Introduction

Triglyceride (TG) is a type of essential natural fats present in the bloodstream, contributing to the delivery of dietary fats through blood vessels [1]. TG concentration levels are classified as normal (TG concentration < 150 mg/dL), borderline (150 mg/dL $\leq$ TG concentration $\leq$ 199 mg/dL), and high (200 mg/dL $\leq$ TG concentration), which is defined as hypertriglyceridemia (HTG) [1]. While TG is a fundamental component in the blood, elevated TG levels pose risks for various diseases, including atherosclerotic cardiovascular disease, low-grade inflammation, pancreatitis, and Alzheimer's disease, due to abnormalities in endothelial function and lipid metabolism [2–4]. Thus, regardless of the underlying causes of HTG, ranging from genetic issues, and dietary habits, to complications from other diseases, appropriate interventions such as lifestyle changes or medical treatments are necessary to reduce TG concentrations to the normal level. Monitoring TG concentration is crucial for diagnosing HTG and assessing the efficacy of interventions.

* Corresponding author at: Global College, Shanghai Jiao Tong University, Shanghai 200240, China.
** Corresponding author at: Department of Mechatronics and Robotics, School of Advanced Technology, Xi'an Jiaotong-Liverpool University, Suzhou 215123, China.
E-mail addresses: sungliang.chen@sjtu.edu.cn (S.-L. Chen), Myeongsu.Seong@xjtlu.edu.cn (M. Seong).
[1] S. Liang, N. Wan, and G. Chen contributed equally to this work.

https://doi.org/10.1016/j.optlastec.2026.114767
Received 23 June 2025; Received in revised form 12 January 2026; Accepted 14 January 2026
Available online 19 January 2026

Given the importance of monitoring TG concentration, an array of relevant research has been dedicated to this area. Among the most widely investigated methods are biosensors, including electrochemical, conducting polymer, metal oxide, and mid-infrared fiber-optic sensors [1,5]. While conventional biosensor-based methods offer absolute TG concentration measurements, the necessity of sample collection and preprocessing restricts the attainment of continuous or repeated TG concentration measurements using existing biosensors. Additionally, the relatively complicated fabrication process of these sensors presents another disadvantage. These limitations underscore the necessity for the development of new technologies to address the challenges associated with TG concentration monitoring.

In response to the demand, some works involving optical technologies have demonstrated the potential for TG concentration monitoring without the need for sample collection. Among these, various spatial frequency domain imaging (SFDI) techniques have emerged as a promising avenue for lipid monitoring [6–8]. Different SFDI systems with infrared light illumination in the range between 800 and 1300 nm are capable of the noninvasive quantification of lipid and water concentrations in blood through the skin. Despite the potential of SFDI systems, challenges remain in their implementation due to the bulkiness of hardware and the complexity of system configuration. Consequently, the development of a portable version of SFDI systems presents obstacles. In the meantime, we recently explored the application of photoacoustic microscopy (PAM) for TG concentration monitoring [9], demonstrating that the amplitude of the PAM signal increased with higher TG concentrations. Although the feasibility of PAM for monitoring TG concentration changes in mixtures of hemoglobin (Hb) and TG, as well as sheep blood and TG, was established, the PAM study used bulky, high-power pulsed lasers and required contact measurements for ultrasound coupling, which hinders potential clinical translation. Thus, further investigation is warranted to facilitate TG concentration monitoring in clinical settings.

Recognizing the technological gaps in monitoring TG concentration, we propose diffuse optical spectroscopy (DOS) as a promising solution. DOS includes various modalities such as continuous-wave DOS (CW-DOS) [10–12], spatially-resolved DOS (SR-DOS) [13–15], frequency-domain DOS (FD-DOS) [16,17], and time-domain DOS (TD-DOS) [18,19]. In this work, we used CW-DOS to estimate changes in TG concentration. Prior to this work, some previous research has utilized the concept of CW-DOS, specifically spatially-resolved CW-DOS, either theoretically or experimentally, which can potentially be used in estimating TG concentration [20–22]. Iinaga et al. used two source-detector pairs for estimating TG in blood in their preliminary study [20]. They estimated a reduced scattering coefficient using a proposed model as an indicator of TG in humans. However, it was not clearly described how the absorption coefficient was estimated, even though the absorption coefficient is necessary in the proposed model to estimate the reduced scattering coefficient. Meanwhile, Liang and Shimizu employed a quasi-CW-DOS with a chopper and a lock-in amplifier to estimate the reduced scattering coefficient in a tube embedded tissue-mimicking phantom, claiming that the coefficient can serve as an index of TG concentration [21]. Like the study by Iinaga et al., Liang and Shimizu used multiple source-detector pairs and a fixed absorption coefficient in their study. Then, Liang et al. further improved the algorithm developed by Liang and Shimizu, making it more practical by estimating both absorption and reduced scattering coefficients using optical measurement data from multiple source-detector pairs [22]. However, the study by Liang et al. only performed Monte Carlo simulations for validation. Previous studies required multiple source-detector pairs and additional signal processing to estimate the reduced scattering coefficient, which served as an index of TG concentration. Unlike previous studies, we attempted to use diffuse reflectance from a single source-detector pair directly as an index for TG concentration changes. Utilizing a laser diode or LED as the light source and a photodiode as the detector, CW-DOS can be implemented as a portable system for continuous signal monitoring. To confirm the feasibility of diffuse optical monitoring of TG concentration variations, we conducted Monte Carlo simulations with the configurations similar to the samples and the DOS system used in this study. Then, phantom experiments were conducted using a mixture of Hb solution and TG with homogeneous and pig skin surrounding media, employing the DOS system to validate its feasibility for diffuse optical monitoring of TG concentration. *Ex vivo* experiments were also performed using a mixture of sheep blood and TG with a pig skin surrounding medium, representing a more clinically relevant setting. Furthermore, *in vivo* mouse studies were performed to investigate the practical applicability of the technique. The results demonstrate the capability of the DOS system for noninvasive and continuous TG concentration monitoring, holding promise for future applications in human subjects.

2. Methods

2.1. Monte Carlo simulation

To confirm the feasibility of diffuse optical monitoring of TG concentration changes in turbid media, Monte Carlo simulation, a widely utilized statistical approach in biomedical optics, was performed using MCXLAB, an open-source Monte Carlo simulation tool based on MATLAB, specifically MATLAB R2019b (Mathworks) [23]. The simulation was run on a PC equipped with an i7-12700 K CPU (Intel), 64 GB RAM, and Nvidia RTX 3090 (Gigabyte), utilizing a custom MATLAB script. For the simulation scenario, we considered monitoring TG concentration in a blood vessel located near the hand's skin. We modeled the optical properties of the hand (absorption coefficient: 0.06 mm^{-1}; reduced scattering coefficient: 1.62 mm^{-1} at 885 nm) [24] as the surrounding medium [25]. Within the medium, a blood vessel with a 1-mm diameter at a depth of 2 mm (ranging from 1.5 mm to 2.5 mm) was presented. Note that the values of the vessel diameter and depth are within the range of the values used in the literature that evaluates vein imaging systems [25,26]. The source and detector were both set to 1 mm in size, with their centers positioned 4.22 mm apart, considering the physical size of optical patch cords. This separation distance was determined to ensure sufficient probing depth to reach the upper region of the tube, based on both preliminary tests and the theory of diffuse optics [10]. To align simulation parameters with experimental conditions, we tailored the Monte Carlo simulation parameters to match those of the DOS system used in this work. The schematic of the Monte Carlo simulation is illustrated in Fig. 1. In the simulation, 250 million photons were set. Considering the weakening trend of scattering [27], the lower absorption of Hb [27,28], and the higher absorption of lipid [27] with increasing optical wavelength and the spectrometer's quantum efficiency, a wavelength of 885 nm was selected for both simulations and experiments. A wide range of Hb and TG concentrations was examined by varying the absorption and reduced scattering coefficients of the tube. Table 1 summarizes the optical properties investigated in the Monte Carlo simulation, with the absorption and reduced scattering coefficients derived from our Hb measurement data and relevant literature [27,29].

2.2. Diffuse optical spectroscopy

Fig. 2(a) shows the setup of the DOS system, which comprises a broadband tungsten halogen lamp (with a 100 W bulb power and a wavelength range of 420–2500 nm, Bobei Lighting Appliance Processing Plant) coupled with an optical fiber patch cord (1 mm core size, Shenzhen Xinrui Photonics Technology) and a commercial spectrometer (Flame-S-XR1, Ocean Optics) coupled with another optical fiber patch cord. The integration time of the spectrometer was set to 100 ms with signal averages of 64 times to balance the signal acquisition rate and signal-to-noise ratio. The center-to-center distance between the source fiber and the detector fiber was set to 4.22 mm, aligning it with the configuration used in the Monte Carlo simulation. To facilitate

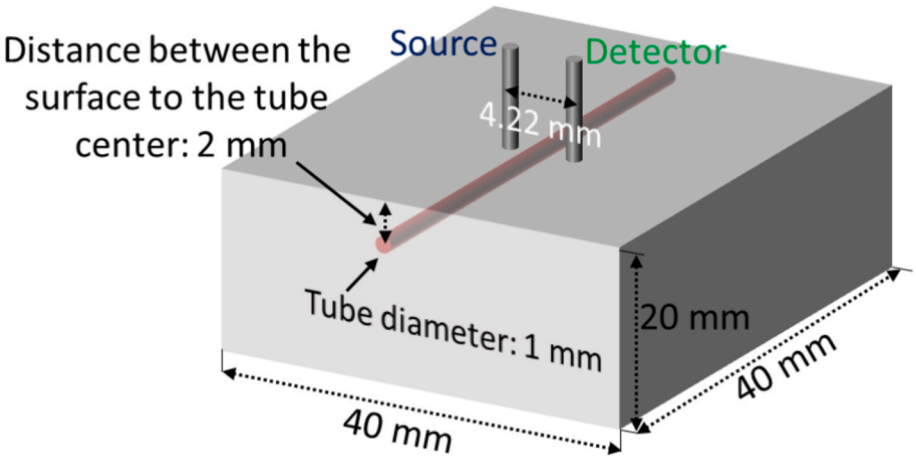

Fig. 1. Schematic setup of Monte Carlo simulation, with a source-detector distance set at 4.22 mm.

Table 1
Concentrations of Hb and TG, along with corresponding absorption and reduced scattering coefficients used in Monte Carlo simulations and phantom experiments.

Hb		TG	
Concentration (mg/mL)	Absorption coefficient (mm^{-1})	Concentration (mg/dL)	Reduced scattering coefficient (mm^{-1})
100	0.44	0	Very small (10^{-6})
125	0.55	200	0.20
150	0.66	400	0.39
175	0.77	600	0.59
200	0.88	800	0.79

experimentation, the fiber probe containing both the source and detector fibers was fixed on a motorized linear stage (M-L01.2A1, Physik Instrumente) to allow easy adjustment of the position of the probe. Signals acquired from the tube samples for both phantom and *ex vivo* experiments (See Section 2.3) were recorded and stored on the PC. Specifically, signal amplitude at 885 nm, consistent with the parameters of the Monte Carlo simulation, was used for following analysis.

2.3. Phantom and ex vivo experiments

To demonstrate the effectiveness of DOS in monitoring TG concentration variations, we conducted experiments using samples with two distinct surrounding media: one with a homogeneous surrounding medium and another with pig skin. The experimental setups are shown in Fig. 2(b) and 2(c), respectively.

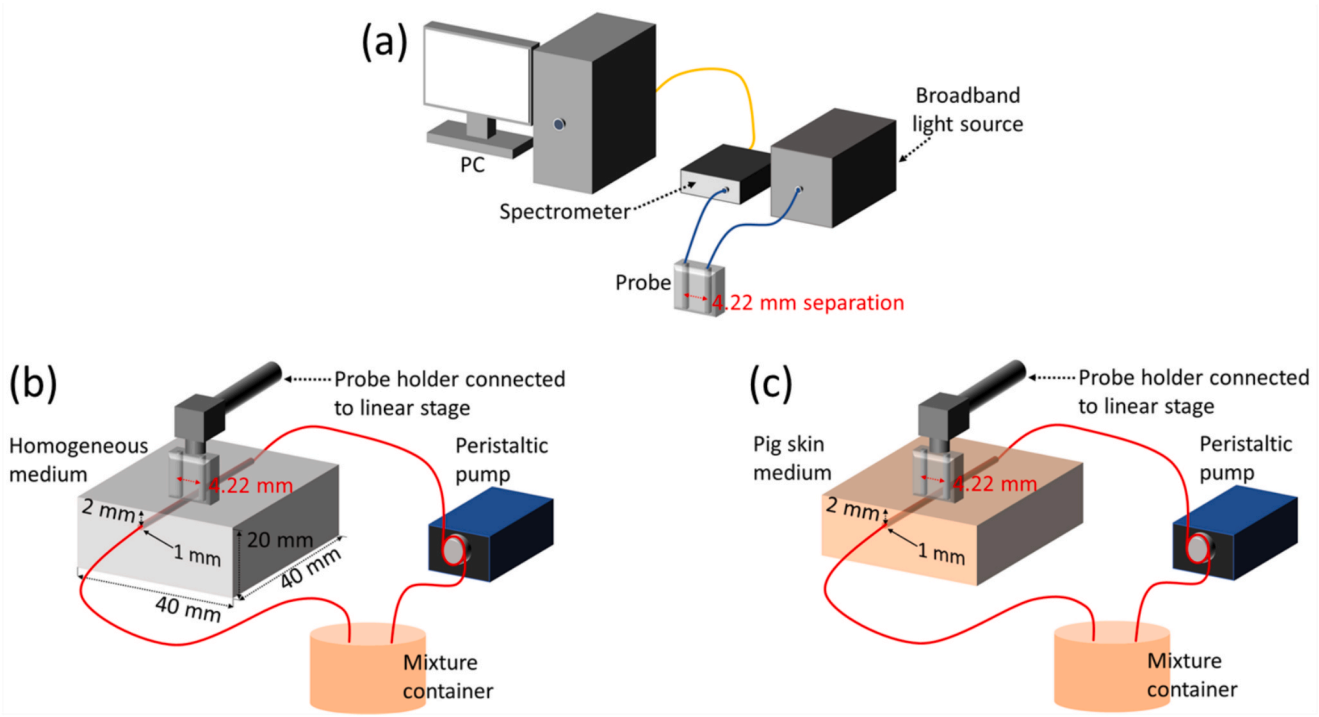

Fig. 2. (a) Schematic of the DOS system used in this work. (b) Schematic of the setup with a homogeneous surrounding medium. The term "Mixture" refers to the mixture of Hb solution and TG. (c) Schematic of the setup with a pig skin surrounding medium. Again, "Mixture" denotes either the mixture of Hb solution and TG or the mixture of sheep blood and TG. In both (b) and (c), the distance between the sample's surface and the tube's center was set to approximately 2 mm, with a tube diameter of 1 mm. The source-detector distance was set to 4.22 mm throughout the experiments.

In the setup with a homogeneous surrounding medium (Fig. 2(b)), a tube (inner diameter: 1 mm; outer diameter: 1.3 mm, Shanghai Jingyu Plastic Products) connected to a peristaltic pump (One China Road Fluid Technology) was embedded in a container. The peristaltic pump was used to mimic the blood flow in the body. The homogeneous medium (absorption coefficient: 0.06 mm^{-1} and reduced scattering coefficient: 1.62 mm^{-1} at 885 nm) [24], comprising intravenous fat emulsion (20 % intralipid, Fresenius Kabi), ink (black ink, rOtring), and water, was filled in the container to mimic tissue properties. For simplicity, we referred to the intravenous fat emulsion as TG. To mimic varying concentrations of Hb (R010156, Rhawn) and TG, mixtures with different concentrations of Hb and TG, as detailed in Table 1, were delivered to the tube embedded in the homogeneous medium using the peristaltic pump.

In the setup with a pig skin surrounding medium (Fig. 2(c)), which is designed for more realistic conditions, we conducted experiments using two samples (described below). In both cases, the tube connected to the peristaltic pump was embedded in a piece of pork, and a surface-to-tube center distance of approximately 2 mm was maintained, consistent with the simulation and the experiments in Fig. 2(b). Similarly, the peristaltic pump was used to mimic the blood flow in the body. Note that pig skin is widely used in biomedical research due to its similarities to human skin [30–32]. In the first sample, similarly, mixtures with concentrations of Hb and TG, as shown in Table 1, were tested for phantom experiments. In the second sample, recognizing the differences between the Hb-based mixture used for blood mimicry and real blood, heparinized sheep blood (Shanghai Yuanye Biotechnology) mixed with varying concentrations of TG, as detailed in Table 1, was employed for *ex vivo* experiments. It is worth noting that the estimation of TG concentration in sheep blood poses greater challenges due to the existence of additional components in the blood such as serum [9].

2.4. In vivo animal experiments

Eight-week-old BALB/c mice (n = 10) were employed to evaluate the effects of TG concentration changes on diffuse reflectance using DOS. The mice were anesthetized with a mixture of 1 % isoflurane and air using an isoflurane anesthesia machine (R500IP, RWD Life Science, China) and an air pump (R510-29, RWD Life Science, China). The fiber probe was positioned over the vascularized dorsal region of the depilated mice. The mice that received saline administration (0.2 mL, 0.9 %) via tail vein injection served as the control group (n = 5). The other mice (n = 5) were administered triton WR-1339, a hyperlipidemic agent (dose: 0.2 mL (500 mg/kg)) [33–37], via tail vein injection to induce the increase in TG concentrations. Among various chemicals, triton WR-1339 was used in the study due to its wide usage for increasing TG concentrations in animal studies [33–37]. Diffuse reflectance signals were measured for 120 min following injection. The spectrometer integration time was set to 450 ms with signal averaging of 100 times (one spectrum acquired approximately every 4.5 s) to minimize fluctuation noise caused by breathing.

3. Results

3.1. Monte Carlo simulation

Fig. 3 shows the results of Monte Carlo simulations. Regardless of the Hb concentration, an increase in TG concentration led to a decrease in normalized diffuse reflectance, which can be attributed to the rise in the overall absorption coefficient within the tube. Notably, variations in Hb concentration solely influenced the overall diffuse reflectance (Fig. 3(a)) without altering the observed trend of decreasing reflectance with increasing TG concentration. For better comparison, the diffuse reflectance data for various Hb concentrations were normalized by the diffuse reflectance obtained at 0 mg/dL TG concentration for each respective Hb concentration (Fig. 3(b)). To further evaluate the data trend, regression analysis was conducted using a linear equation of the form 'y = ax + b'. The coefficients of determination (R^2) for the regression results exceeded 0.99, indicating a robust fit of the data to the linear model. The compelling results obtained from the Monte Carlo simulation motivated us to proceed with further experimentation, focusing on diffuse optical monitoring of TG concentration changes in a few samples.

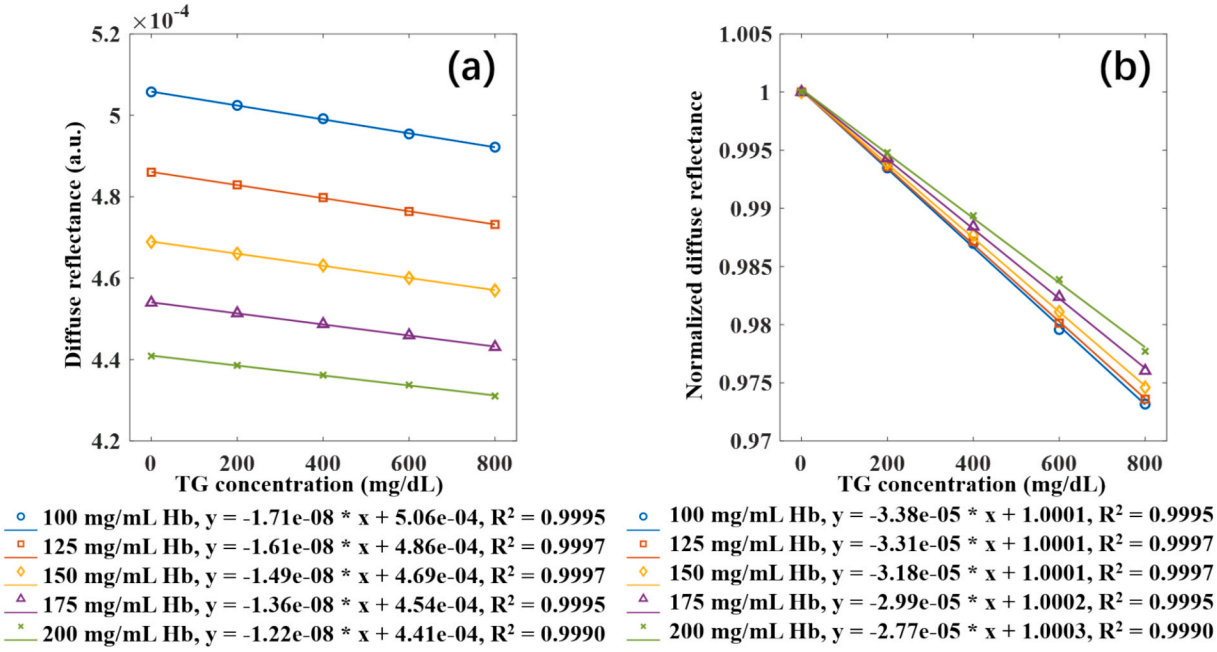

Fig. 3. (a) Diffuse reflectance and (b) normalized diffuse reflectance of Monte Carlo simulation. The data were fitted using a linear equation 'y = ax + b', where 'y' represents the normalized diffuse reflectance and 'x' stands for the TG concentration. In this equation, 'a' denotes the rate or slope of the change, while 'b' means the y-intercept. The coefficient of determination (R^2) quantifies the goodness of fit of the data to the linear equation. A value of $R^2 = 1$ indicates a perfect fit to the linear equation, while $R^2 = 0$ suggests no relationship between the data and the equation. The diffuse reflectance signals of different Hb concentrations exhibit a linear decrease with increasing TG concentration.

3.2. Phantom and ex vivo experiments

Fig. 4 shows the results obtained from the samples containing mixtures of Hb and TG embedded within the homogeneous surrounding medium. Regardless of Hb concentration, an increase in TG concentration corresponded to a decrease in diffuse reflectance (Fig. 4(a)). Similarly, for better comparison, the diffuse reflectance data for various Hb concentrations were normalized by the diffuse reflectance observed at 0 mg/dL TG concentration for each respective Hb concentration (Fig. 4 (b)). The trend aligns closely with the findings of the Monte Carlo simulation. Regression analysis was also performed on the normalized diffuse reflectance signals using a linear equation, and R^2 for the regression of all the data exceeded 0.99.

Fig. 5(a) and 5(b) present the raw diffuse reflectance and normalized diffuse reflectance obtained from the samples containing mixtures of Hb and TG embedded within the pig skin surrounding medium, respectively. Similar to the previous analyses, the diffuse reflectance data for different Hb concentrations were normalized by the diffuse reflectance observed at 0 mg/dL TG concentration for each respective Hb concentration. Consistently, regardless of Hb concentration, an increase in TG concentration resulted in a decrease in normalized diffuse reflectance. Meanwhile, an increase in Hb concentration similarly reduced the overall amplitude of raw diffuse reflectance (Fig. 5(a)). Regression analysis was performed using a linear equation, and R^2 for the regression of all data exceeded or closely approached 0.99. Despite the slopes of the curves being mostly lower in Fig. 5(b) compared to Fig. 4(b) for each corresponding Hb concentration, except the case of 150 mg/mL Hb concentration, the linear relationship between the normalized diffuse reflectance signals and TG concentrations remained consistent across all tested Hb concentrations.

Fig. 5(c) and (d) show the raw diffuse reflectance and normalized diffuse reflectance obtained from the samples containing mixtures of sheep blood and TG embedded within the pig skin surrounding medium, respectively. Notably, a similar trend was observed when sheep blood was used instead of the blood solution based on Hb powder. Linear regression analysis revealed that the linear relationship between the diffuse reflectance signals and TG concentrations remained, with R^2 values of the regression exceeding 0.99. This consistency underscores the robustness of the method even with the use of sheep blood. The use of sheep blood instead of Hb powder, as well as the pig skin surrounding medium, enhances the relevance of the experimental conditions to clinical scenarios. The strong linearity observed in Fig. 5(c) and 5(d) underscore the potential for TG concentration monitoring in complex blood using the straightforward DOS configuration.

3.3. In vivo animal experiments

Fig. 6 shows the results (mean ± standard deviation) obtained from *in vivo* animal experiments. In the first 35 min post-injection, while both the saline-administered group and the triton-administered group showed a drop in normalized diffuse reflectance, the triton-administered group showed a more prominent decrease in normalized diffuse reflectance than that of the saline-administered group. After 35 min, normalized diffuse reflectance in the saline-administered group did not show any significant change, while that of the triton-administered group continually decreased until the end of the experiment, which is due to the increase in TG concentrations caused by the triton administration. The results of the *in vivo* animal experiments show the potential of DOS in the longitudinal monitoring of TG concentrations in individuals.

For comparison, a study by Lin et al. reported that plasma TG levels increased from 173.8 mg/dL to approximately 1000 mg/dL within 120 min following administration of triton WR-1339 at a dose of 500 mg/kg [38]. Based on the fitted linear equations derived from the pig skin phantom experiments, specifically, y = -3.53e-0.5 × 'TG concentration' + 1.0014 for 125 mg/mL Hb and y = -3.88e-0.5 × 'TG concentration' + 0.9999 for 150 mg/mL Hb (see Fig. 5(b)), the estimated normalized diffuse reflectance signals corresponding to TG concentrations of 173.8 mg/dL and 1000 mg/dL are approximately 0.9942 and 0.9636, respectively, assuming an intermediate Hb concentration of 137.5 mg/mL. Considering that the Hb concentration in mice is approximately 134 mg/mL [39], the change in normalized diffuse reflectance observed in our *in vivo* experiments following triton WR-1339 administration, from 1

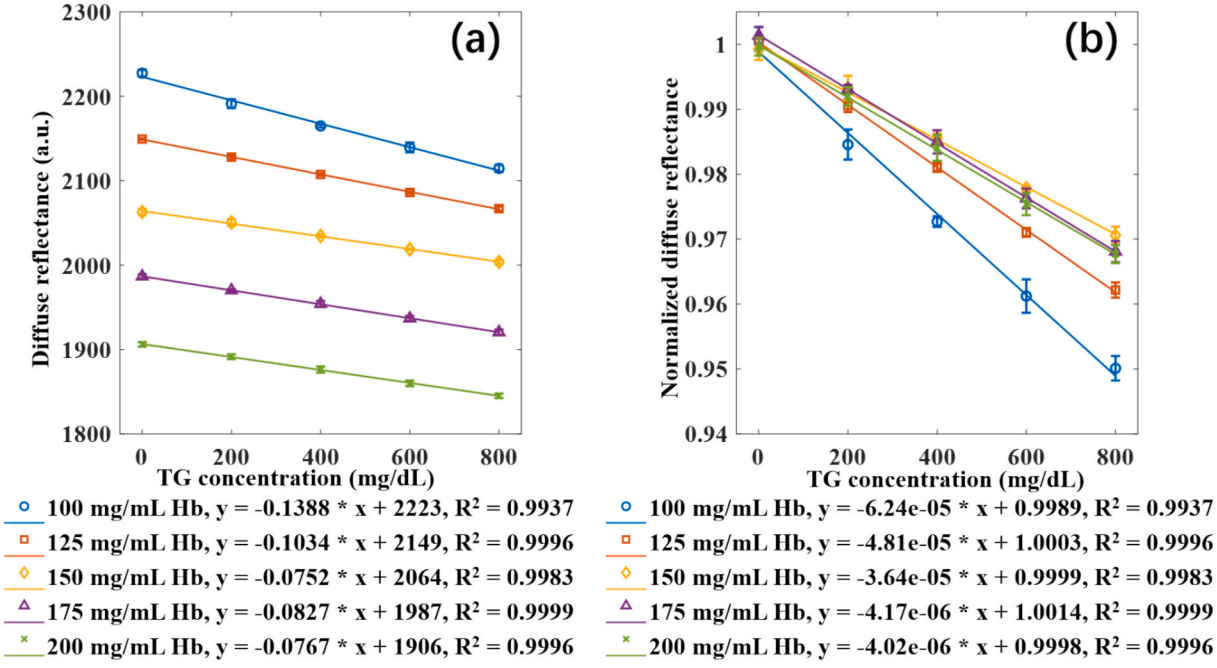

Fig. 4. (a) Raw diffuse reflectance and (b) normalized diffuse reflectance from the samples containing mixtures of Hb and TG embedded within the homogeneous surrounding medium. The mean and standard deviation (error bars) were calculated from three independently acquired spectra. The data were fitted to a linear equation 'y = ax + b', where 'y', 'x', 'a', and 'b' are mentioned in the caption of Fig. 3. Besides, R^2 is also described in the caption of Fig. 3. The diffuse reflectance signals of different Hb concentrations exhibit a linear decrease with increasing TG concentration.

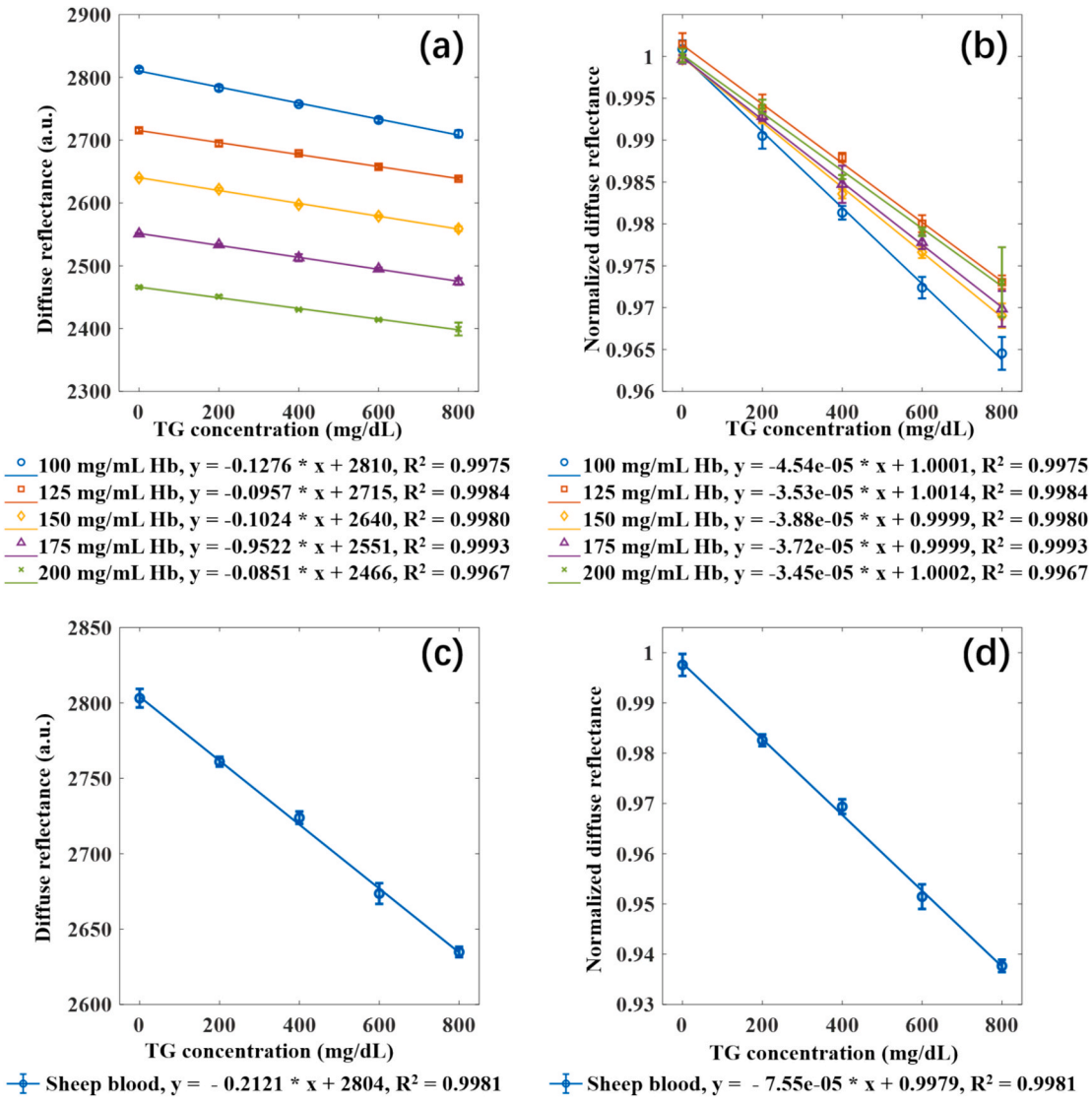

Fig. 5. (a) Raw diffuse reflectance and (b) normalized diffuse reflectance from the samples containing mixtures of Hb and TG embedded within the pig skin surrounding medium. (c) Raw diffuse reflectance and (d) normalized diffuse reflectance from the samples containing mixtures of sheep blood and TG embedded within the pig skin surrounding medium. The mean and standard deviation (error bars) were calculated from three independently acquired spectra. The data were fitted to a linear equation 'y = ax + b', where 'y', 'x', 'a', and 'b' are mentioned in the caption of Fig. 3, except that in (c) and (d), 'x' stands for the added TG concentration to the sheep blood. Besides, R^2 is also described in the caption of Fig. 3. In (a)–(d), the diffuse reflectance signals exhibit a linear decrease with increasing TG concentration.

to ~ 0.956 (see Fig. 6), falls within the expected range compared with the estimations derived from Lin et al.'s results [38]. Here, the outcome is subject to alternative interpretation because a compounding factor may exist in the diffuse reflectance signal changes, as the saline injection group also showed a decrease in normalized diffuse reflectance from 1 to ~ 0.99. If the change caused by saline injection is incorporated, the change of the normalized diffuse reflectance signals at 120 min can be considered ~ 0.946, not ~ 0.956. In this case, the outcome can be interpreted as an overestimation of the variation in TG concentration in the *in vivo* experiment (overestimated the change as 5.5 % from 4.4 %); however, it still does not alter the fact that the proposed technique is capable of monitoring TG variation without requiring sample collection. Instead, this suggests that more advanced systems, which can decouple the influence of optical absorption and scattering on diffuse reflectance, would be necessary to more accurately monitor the TG variation as described in the Discussions section.

4. Discussions

In this study, we successfully demonstrated that CW-DOS is capable of monitoring TG concentration variations. To thoroughly validate the feasibility of DOS in longitudinal monitoring of TG concentration variations, this work employed Monte Carlo simulations along with phantom, *ex vivo*, and *in vivo* experiments. To mimic the conditions of *in vivo* measurement of the subsurface vein under the skin of the arm or hand, we conducted experiments using flowing mixtures of sheep blood and varying concentrations of TG embedded within the pig skin surrounding medium. The choice of *ex vivo* pig skin lies in its widespread use for validating optical systems intended for eventual *in vivo* applications, along with the similarities between pig skin and human skin tissue in terms of both optical properties and structure [30–32]. Additionally, the utilization of the peristaltic pump to maintain a continuous flow of sheep blood during measurements can mimic the pulsatile nature of blood flow caused by the heartbeat and the presence of plasma affecting diffuse optical measurements [9]. To further assess the potential of the

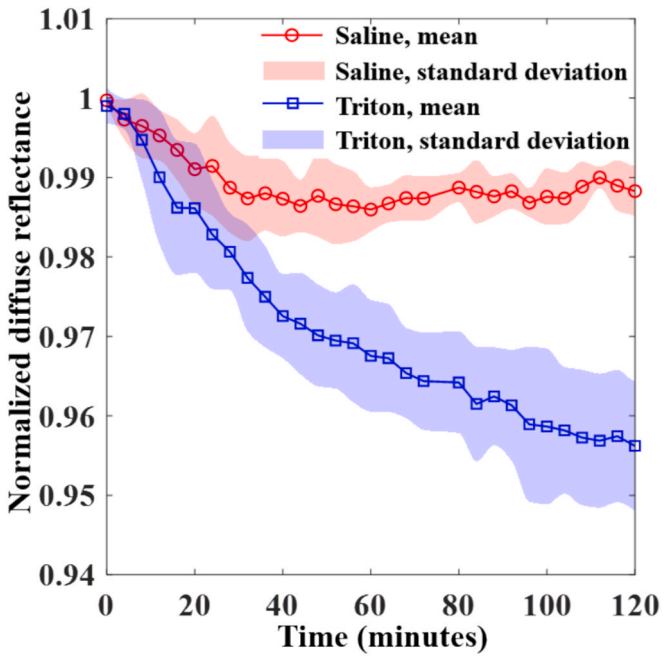

Fig. 6. Changes in diffuse reflectance of the dorsal region of mice following injection of saline (red) and triton WR-1339 (blue) over 120 min (mean: lines with markers; standard deviation: shaded regions). The mean and standard deviation were calculated from data obtained from five mice in each group.

proposed technique for *in vivo* applications, an animal study was conducted, comprising a saline-administered group (n = 5) and a triton-administered group (n = 5). Moving toward clinical studies, the differential response of diffuse optical signals from a subsurface blood vessel should be compared against other TG biosensors or conventional techniques, under varied lipid intake during meal consumption [6,20]. Such comparative analyses will contribute to the validation of DOS efficacy in real-world scenarios, offering valuable insights into its potential clinical utility. Another point to consider is the use of an animal model with pathological conditions. In the current study, healthy animals were used to demonstrate the feasibility of longitudinal TG monitoring. However, the physiological response in animals or humans with pathological conditions, such as liver or kidney diseases [40,41], can differ from that of healthy individuals. Thus, further investigations with diseased animal models are warranted to more comprehensively validate the applicability of the proposed technique in broader situations.

The results of our *ex vivo* experiment using sheep blood (Fig. 5(c) and 5(d)) and the *in vivo* animal experiments (Fig. 6) demonstrate trends that closely align with those observed in the Monte Carlo simulations (Fig. 3). The consistency further supports the validity of our assumptions in the simulation and suggests that the discrepancies between the simulation and real experiments are minimal. While the technique's sensitivity to low TG concentrations (< 150 mg/dL TG) has not been explicitly demonstrated in simulations and experiments, because this technique is intended to monitor HTG, monitoring the variation of TG concentration within the normal range (<150 mg/dL) is still feasible, as partially evidenced by the small error bars in Fig. 4(b) and 5(d). The minimum detectable variation in TG concentration could be further improved by increasing the signal-to-noise ratio of the diffuse reflectance measurements. Potential approaches include averaging more than 64 acquisitions at the expense of sampling frequency, or utilizing a detector with higher quantum efficiency and/or lower intrinsic noise than the one used in this study.

Our primary objective is to develop a technique capable of longitudinal monitoring of TG concentrations in individuals. This capability is experimentally demonstrated using a mouse model, as shown in Fig. 6. The mean Hb concentrations for young adult females and males are 129.7 mg/mL and 160.3 mg/mL, respectively. According to a previous study [42], the intra-subject variation in Hb concentrations is relatively small, which is only 2.74 % on average over 10 weeks. As shown in Figs. 3-5, such a minimal variation in Hb concentrations does not result in a significant change in diffuse reflectance. Therefore, while further rigorous preclinical and clinical studies are warranted, our method shows potential for intra-subject measurement of TG concentrations.

Owing to the ease of access, this work assumed monitoring of TG concentration variations within the subsurface veins of the hand or arm, which are easily discernible to the naked eye. Among the veins of the human body, these veins are particularly accessible due to their lower light scattering compared to thicker tissues. However, translating this technology into human measurements presents potential challenges. Firstly, skin color, determined by melanin concentration, may affect measurements [24,27]. Secondly, variations in body fat levels in tissues may also impact accuracy [14,43–45]. Both melanin and body fat influence the absorption and scattering coefficients at the measurement site, which are crucial factors in diffuse optical measurements. Other chromophores, including water, may also influence the measurement, as shown in Section 3.3. Thus, further investigation is warranted to assess the effects of increased absorption and scattering coefficients in the surrounding medium.

Among various DOS systems available, this study utilized CW-DOS, which solely monitors relative amplitude changes. This configuration holds promise for conversion into a portable system using either an LED or a laser diode as the light source and a photodiode as the detector. With an appropriate calibration procedure, such as compensating for the effect of skin optical properties by utilizing DOS signals measured longitudinally, this configuration could evolve into a personalized monitoring device. Such a development would be groundbreaking, considering the current absence of a personalized, continuous TG concentration monitoring device. Exploring the potential of more complicated DOS systems, such as SR-DOS, FD-DOS, and TD-DOS, in TG concentration monitoring is essential. These systems offer the possibility of providing absolute TG concentrations and compensating for influences from Hb variation, melanin, and body fat due to their quantification abilities [14,16]. Additionally, leveraging artificial intelligence techniques, including machine learning and deep learning [46,47], holds promise for maximizing the utility of multi-wavelength spectra (rather than the single 885-nm wavelength used in this study), which could effectively integrate information from the probed region, including blood vessels and surrounding tissue, into the analysis.

The development of multi-modal systems for TG concentration monitoring is another exciting research direction. In our previous study, we demonstrated the feasibility of PAM in TG concentration monitoring [9]. Due to the fact that DOS systems utilize signals from back-reflected photons after experiencing multiple scatterings, these signals can be influenced by surrounding blood vessels. Unlike DOS systems, PAM offers the capability to precisely pinpoint surrounding blood vessels. Combining PAM and DOS systems presents a promising approach to mitigate the impact of surrounding tissues. Specifically, PAM can visualize the surrounding blood vessels, and Monte Carlo simulations with visualized blood vessels can be performed to compensate for the influence of the surrounding blood vessels on DOS measurements. This synergistic combination holds significant potential for enhancing the accuracy and reliability of TG concentration measurements.

5. Conclusion

In conclusion, we demonstrated TG concentration monitoring utilizing the simplest DOS configuration, CW-DOS, which includes a continuous broadband light source and a spectrometer. Through Monte Carlo simulations and experiments using the phantom and *ex vivo* samples, notably those containing mixtures of sheep blood and TG embedded within the pig skin surrounding medium, we have demonstrated the feasibility of diffuse optical monitoring of TG concentration

variations, where a subsurface vein of the arm was assumed. Additionally, *in vivo* animal experiments were performed to demonstrate the applicability of the technique. While further clinical studies are warranted for validation, our results show promising prospects for diffuse optical monitoring of TG concentration. Thus, we believe that this work will open up a new opportunity for various types of DOS in TG concentration monitoring.

CRediT authorship contribution statement

Siqi Liang: Writing – original draft, Validation, Software, Methodology, Investigation, Data curation. **Nan Wan:** Methodology, Investigation, Formal analysis, Conceptualization. **Guo Chen:** Methodology, Investigation, Formal analysis, Conceptualization. **Sung-Liang Chen:** Writing – review & editing, Supervision, Resources, Funding acquisition, Formal analysis. **Myeongsu Seong:** Writing – review & editing, Writing – original draft, Visualization, Supervision, Methodology, Investigation, Data curation.

Declaration of competing interest

The authors declare that they have no known competing financial interests or personal relationships that could have appeared to influence the work reported in this paper.

Acknowledgments

This research was partially supported by the Research Development Fund of Xi'an Jiaotong-Liverpool University (RDF-23-01-119), the Natural Science Foundation of Jiangsu Province (BK20220603), the National Natural Science Foundation of China (62235013 and 82130057), the Science and Technology Commission of Shanghai Municipality (20DZ2220400 and 2021SHZDZX), the Natural Science Foundation of Hunan Province (2025JJ70638), and the Scientific Research Fund of Hunan Provincial Education Department (24C0233).

Data availability

Data will be made available on request.

References

[1] C.S. Pundir, V. Narwal, Biosensing methods for determination of triglycerides: a review, Biosens. Bioelectron. 100 (2018) 214–227, https://doi.org/10.1016/j.bios.2017.09.008.
[2] C.S. Pundir, B. Sandeep Singh, J. Narang, Construction of an amperometric triglyceride biosensor using PVA membrane bound enzymes, Clin. Biochem. 43 (2010) 467–472, https://doi.org/10.1016/j.clinbiochem.2009.12.003.
[3] U. Laufs, K.G. Parhofer, H.N. Ginsberg, R.A. Hegele, Clinical review on triglycerides, Eur. Heart J. 41 (2020) 99–109c, https://doi.org/10.1093/eurheartj/ehz785.
[4] L. Tokgözoğlu, P. Libby, The dawn of a new era of targeted lipid-lowering therapies, Eur. Heart J. 43 (2022) 3198–3208, https://doi.org/10.1093/eurheartj/ehab841.
[5] S. Zhou, X. Li, J. Zhang, H. Yuan, X. Hong, Y. Chen, Dual-fiber optic bioprobe system for triglyceride detection using surface plasmon resonance sensing and lipase-immobilized magnetic bead hydrolysis, Biosens. Bioelectron. 196 (2022) 113723, https://doi.org/10.1016/j.bios.2021.113723.
[6] Y. Zhao, A. Pilvar, A. Tank, H. Peterson, J. Jiang, J.C. Aster, J.P. Dumas, M. C. Pierce, D. Roblyer, Shortwave-infrared meso-patterned imaging enables label-free mapping of tissue water and lipid content, Nat. Commun. 11 (2020) 5355, https://doi.org/10.1038/s41467-020-19128-7.
[7] A. Pilvar, J. Plutzky, M.C. Pierce, D. Roblyer, Shortwave infrared spatial frequency domain imaging for non-invasive measurement of tissue and blood optical properties, J. Biomed. Opt. 27 (2022), https://doi.org/10.1117/1.JBO.27.6.066003.
[8] B. Song, X. Yin, Y. Fan, Y. Zhao, Quantitative spatial mapping of tissue water and lipid content using spatial frequency domain imaging in the 900- to 1000-nm wavelength region, J. Biomed. Opt. 27 (2022), https://doi.org/10.1117/1.JBO.27.10.105005.
[9] N. Wan, Z. Li, M. Seong, K. Zhang, W. Niu, R. Wu, S.-L. Chen, Sensing of triglyceride concentration in blood solution using photoacoustic microscopy, Opt. Lett. 48 (2023) 3769, https://doi.org/10.1364/OL.485194.
[10] M. Seong, Y. Oh, H.J. Park, W.-S. Choi, J.G. Kim, Use of hypoxic respiratory challenge for differentiating Alzheimer's disease and wild-type mice non-invasively: a diffuse optical spectroscopy study, Biosensors 12 (2022) 1019, https://doi.org/10.3390/bios12111019.
[11] M. Seong, Z. Phillips, P.M. Mai, C. Yeo, C. Song, K. Lee, J.G. Kim, Simultaneous blood flow and blood oxygenation measurements using a combination of diffuse speckle contrast analysis and near-infrared spectroscopy, J. Biomed. Opt. 21 (2016) 027001, https://doi.org/10.1117/1.JBO.21.2.027001.
[12] M. Seong, P.M. Mai, K. Lee, J.G. Kim, Simultaneous blood flow and oxygenation measurements using an off-the-shelf spectrometer, Chin. Opt. Lett. 16 (2018) 071701, https://doi.org/10.3788/COL201816.071701.
[13] T. Li, M. Duan, K. Li, G. Yu, Z. Ruan, Bedside monitoring of patients with shock using a portable spatially-resolved near-infrared spectroscopy, Biomed. Opt. Express 6 (2015) 3431, https://doi.org/10.1364/BOE.6.003431.
[14] V.M. Niemeijer, J.P. Jansen, T. Van Dijk, R.F. Spee, E.J. Meijer, H.M.C. Kemps, P.F. F. Wijn, The influence of adipose tissue on spatially resolved near-infrared spectroscopy derived skeletal muscle oxygenation: the extent of the problem, Physiol. Meas. 38 (2017) 539–554, https://doi.org/10.1088/1361-6579/aa5dd5.
[15] L. Zhang, M. Sun, Z. Wang, H. Li, Y. Li, G. Li, L. Lin, Noncontact blood species identification method based on spatially resolved near-infrared transmission spectroscopy, Infrared Phys. Technol. 85 (2017) 32–38, https://doi.org/10.1016/j.infrared.2017.05.011.
[16] X. Zhou, Y. Xia, J. Uchitel, L. Collins-Jones, S. Yang, R. Loureiro, R.J. Cooper, H. Zhao, Review of recent advances in frequency-domain near-infrared spectroscopy technologies, Biomed. Opt. Express 14 (2023) 3234, https://doi.org/10.1364/BOE.484044.
[17] A. Kılıç, Y. Miao, V. Koomson, Design of a miniaturized frequency domain near infrared spectrometer with validation in solid phantoms and human tissue, J. Near Infrared Spectrosc. 31 (2023) 3–13, https://doi.org/10.1177/09670335221134206.
[18] G. Giacalone, M. Zanoletti, R. Re, B. Germinario, D. Contini, L. Spinelli, A. Torricelli, L. Roveri, Time-domain near-infrared spectroscopy in acute ischemic stroke patients, Neurophotonics 6 (2019) 015003, https://doi.org/10.1117/1.NPh.6.1.015003.
[19] M. Lacerenza, M. Buttafava, M. Renna, A.D. Mora, L. Spinelli, F. Zappa, A. Pifferi, A. Torricelli, A. Tosi, D. Contini, Wearable and wireless time-domain near-infrared spectroscopy system for brain and muscle hemodynamic monitoring, Biomed. Opt. Express 11 (2020) 5934, https://doi.org/10.1364/BOE.403327.
[20] K. Iinaga, T. Namita, T. Sakurai, H. Chiba, K. Shimizu, Attempt for noninvasive evaluation of in vivo triglyceride in blood, in: 2013 35th Annual International Conference of the IEEE Engineering in Medicine and Biology Society (EMBC), IEEE, Osaka, 2013, pp. 1214–1217, https://doi.org/10.1109/EMBC.2013.6609725.
[21] S. Liang, K. Shimizu, Development of a technique to measure local scattering in turbid media using backscattered light at the surface for noninvasive turbidity evaluation of blood in subcutaneous blood vessels, Jpn. J. Appl. Phys. 60 (2021) 022002, https://doi.org/10.35848/1347-4065/abd36a.
[22] S. Liang, T. Miyake, K. Shimizu, Optical parameters estimation in inhomogeneous turbid media using backscattered light: for transcutaneous scattering measurement of intravascular blood, Biomed. Opt. Express 15 (2024) 237, https://doi.org/10.1364/BOE.510245.
[23] Q. Fang, D.A. Boas, Monte Carlo simulation of photon migration in 3D turbid media accelerated by graphics processing units, Opt. Express 17 (2009) 20178, https://doi.org/10.1364/OE.17.020178.
[24] S.-H. Tseng, A. Grant, A.J. Durkin, In vivo determination of skin near-infrared optical properties using diffuse optical spectroscopy, J. Biomed. Opt. 13 (2008) 014016, https://doi.org/10.1117/1.2829772.
[25] C.A. Mela, D.P. Lemmer, F.S. Bao, F. Papay, T. Hicks, Y. Liu, Real-time dual-modal vein imaging system, Int. J. Comput. Assist. Radiol. Surg. 14 (2019) 203–213, https://doi.org/10.1007/s11548-018-1865-9.
[26] N.J. Cuper, J.H.G. Klaessens, J.E.N. Jaspers, R. De Roode, H.J. Noordmans, J.C. De Graaff, R.M. Verdaasdonk, The use of near-infrared light for safe and effective visualization of subsurface blood vessels to facilitate blood withdrawal in children, Med. Eng. Phys. 35 (2013) 433–440, https://doi.org/10.1016/j.medengphy.2012.06.007.
[27] S.L. Jacques, Optical properties of biological tissues: a review, Phys. Med. Biol. 58 (2013) R37–R61, https://doi.org/10.1088/0031-9155/58/11/R37.
[28] M. Seong, S.-L. Chen, Recent advances toward clinical applications of photoacoustic microscopy: a review, Sci. China Life Sci. 63 (2020) 1798–1812, https://doi.org/10.1007/s11427-019-1628-7.
[29] H.J. van Staveren, C.J.M. Moes, J. van Marie, S.A. Prahl, M.J.C. van Gemert, Light scattering in Intralipid-10% in the wavelength range of 400-1100 nm, Appl. Opt. 30 (1991) 4507–4514, https://doi.org/10.1364/AO.30.004507.
[30] A.P.M. Michel, S. Liakat, K. Bors, C.F. Gmachl, In vivo measurement of mid-infrared light scattering from human skin, Biomed. Opt. Express 4 (2013) 520, https://doi.org/10.1364/BOE.4.000520.
[31] E. Zamora-Rojas, B. Aernouts, A. Garrido-Varo, W. Saeys, D. Pérez-Marín, J. E. Guerrero-Ginel, Optical properties of pig skin epidermis and dermis estimated with double integrating spheres measurements, Innov. Food Sci. Emerg. 20 (2013) 343–349, https://doi.org/10.1016/j.ifset.2013.06.008.
[32] T.P. Sullivan, W.H. Eaglstein, S.C. Davis, P. Mertz, The pig as a model for human wound healing, Wound Repair Regen. 9 (2001) 66–76, https://doi.org/10.1046/j.1524-475x.2001.00066.x.
[33] Z. Chen, R.L. Fitzgerald, M.R. Averna, G. Schonfeld, A targeted apolipoprotein B-38.9-producing mutation causes fatty livers in mice due to the reduced ability of apolipoprotein B-38.9 to transport triglycerides, J. Biol. Chem. 275 (2000) 32807–32815, https://doi.org/10.1074/jbc.M004913200.

[34] J.R. Goudriaan, M.A.M. Den Boer, P.C.N. Rensen, M. Febbraio, F. Kuipers, J. A. Romijn, L.M. Havekes, P.J. Voshol, CD36 deficiency in mice impairs lipoprotein lipase-mediated triglyceride clearance, J. Lipid Res. 46 (2005) 2175–2181, https://doi.org/10.1194/jlr.M500112-JLR200.
[35] J.S. Millar, D.A. Cromley, M.G. McCoy, D.J. Rader, J.T. Billheimer, Determining hepatic triglyceride production in mice: comparison of poloxamer 407 with Triton WR-1339, J. Lipid Res. 46 (2005) 2023–2028, https://doi.org/10.1194/jlr.D500019-JLR200.
[36] M. Wu, Q. Wang, H. Li, J. Tao, Z. Wang, S. Zhang, L. Chen, P. Li, L. Chen, L. Qu, PLA2G12A protects against diet-induced obesity and insulin resistance by enhancing energy expenditure and clearance of circulating triglycerides, FASEB J. 38 (2024) e23643, https://doi.org/10.1096/fj.202302075R.
[37] A.A. Attia, L.M. El-Samad, N. Zaghloul, Effects of protein extract from the housefly larvae (Musca domestica vicina) on the hyperlipidemic mice induced by Triton WR-1339, Swed. J. BioSci. Res. 1 (2020) 16–27, https://doi.org/10.51136/sjbsr.2020.16.27.
[38] X. Lin, P. Yue, Z. Chen, G. Schonfeld, Hepatic triglyceride contents are genetically determined in mice: results of a strain survey, Am. J. Physiol.-Gastrointestinal Liver Physiol. 288 (2005) G1179–G1189, https://doi.org/10.1152/ajpgi.00411.2004.
[39] E.W. Santos, D.C.D. Oliveira, A. Hastreiter, G.B.D. Silva, J.S.D.O. Beltran, M. Tsujita, A.R. Crisma, S.M.P. Neves, R.A. Fock, P. Borelli, Hematological and biochemical reference values for C57BL/6, Swiss Webster and BALB/c mice, Braz. J. Vet. Res. Anim. Sci. 53 (2016) 138, https://doi.org/10.11606/issn.1678-4456.v53i2p138-145.
[40] M. Alves-Bezerra, D.E. Cohen, Triglyceride metabolism in the liver, Compr. Physiol. 8 (2018) 1–22, https://doi.org/10.1002/j.2040-4603.2018.tb00008.x.
[41] S. Zubovic, S. Kristic, S. Pasic, Chronic kidney disease and lipid disorders, Med. Arh. 70 (2016) 191–192, https://doi.org/10.5455/medarh.2016.70.191-192.
[42] A. Coşkun, A. Carobene, M. Kilercik, M. Serteser, S. Sandberg, A.K. Aarsand, P. Fernandez-Calle, N. Jonker, W.A. Bartlett, J. Díaz-Garzón, S. Huet, C. Kızıltaş, I. Dalgakıran, E. Ugur, I. Unsal, Within-subject and between-subject biological variation estimates of 21 hematological parameters in 30 healthy subjects, Clin. Chem. Laborat. Med. (CCLM) 56 (2018) 1309–1318, https://doi.org/10.1515/cclm-2017-1155.
[43] Ö. Şayli, E.B. Aksel, A. Akın, Crosstalk and error analysis of fat layer on continuous wave near-infrared spectroscopy measurements, J. Biomed. Opt. 13 (2008) 064019, https://doi.org/10.1117/1.3028008.
[44] S. Homma, T. Fukunaga, A. Kagaya, Influence of adipose tissue thickness on near infrared spectroscopic signal in the measurement of human muscle, J. Biomed. Opt. 1 (1996) 418, https://doi.org/10.1117/12.252417.
[45] Y. Yang, O. Soyemi, P.J. Scott, M.R. Landry, S.M. Lee, L. Stroud, B.R. Soller, Quantitative measurement of muscle oxygen saturation without influence from skin and fat using continuous-wave near infrared spectroscopy, Opt. Express 15 (2007) 13715, https://doi.org/10.1364/OE.15.013715.
[46] U.M. Pal, M. Saxena, G.K. Anil Vishnu, D. Parsana, B.S.R. Sarvani, M. Varma, M. Jayachandra, V. Kurpad, D. Baruah, G. Gogoi, J.S. Vaidya, H.J. Pandya, Optical spectroscopy-based imaging techniques for the diagnosis of breast cancer: a novel approach, Appl. Spectrosc. Rev. 55 (2020) 778–804, https://doi.org/10.1080/05704928.2020.1749651.
[47] R. Gunaratne, J. Goncalves, I. Monteath, R. Sheh, M. Kapfer, R. Chipper, B. Robertson, R. Khan, D. Fick, C.N. Ironside, Wavelength weightings in machine learning for ovine joint tissue differentiation using diffuse reflectance spectroscopy (DRS), Biomed. Opt. Express 11 (2020) 5122, https://doi.org/10.1364/BOE.397593.